Journal of Hazardous Materials 438 (2022) 129537

Contents lists available at ScienceDirect

Journal of Hazardous Materials

journal homepage: www.elsevier.com/locate/jhazmat

Research Paper

Interaction of peracetic acid with chromium(III): Understanding degradation of coexisting organic pollutants in water

Joshua Bell [a,b], Yinghao Wen [c], Xingmao Ma [c], Thomas J. McDonald [b], Ching-Hua Huang [d,*], Virender K. Sharma [b,*]

[a] Department of Water Management and Hydrological Science, Texas A&M University, College Station, TX 77843, USA
[b] Program for the Environment and Sustainability, Department of Environmental and Occupational Health, School of Public Health, Texas A&M University, 212 Adriance Lab Rd., 1266 TAMU, College Station, TX 77843, USA
[c] Department of Civil and Environmental Engineering, Texas A&M University, College Station, TX 77843, USA
[d] School of Civil and Environmental Engineering, Georgia Institute of Technology, Atlanta, GA 30332, USA

HIGHLIGHTS

- Peracetic acid activation by Cr(III) produces reactive species, $^{\bullet}OH$ and Cr(IV)/Cr(V).
- Reactive intermediate species degrade co-existing pharmaceuticals in water.
- Magnitude of degradation depends on the molecular structure of pharmaceuticals.
- pH dependence of PAA activation is related to $Cr(OH)_3^0$ species.
- Oxidized products of trimethoprim by PAA-Cr(III) and H_2O_2-Cr(III) are similar.

GRAPHICAL ABSTRACT

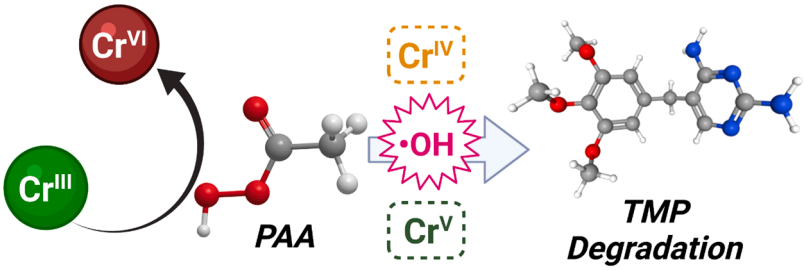

ARTICLE INFO

Editor: Dr. B. Lee

Keywords:
Peroxyacetic acid
Metal ions
Micropollutants
Enhanced degradation
Oxidation products
High-valent chromium

ABSTRACT

Peracetic acid (PAA, $CH_3C(O)OOH$) has gained significant attention for its use in wastewater disinfection. Wastewater usually contains both metal ions and organic pollutants and understanding reactions after adding PAA to such contaminated water is needed. This paper presents results regarding the effect of interactions between chromium(III) (Cr(III)) and PAA on the degradation of selected pharmaceuticals, mainly trimethoprim (TMP). The degradation of pharmaceuticals by PAA, PAA-Cr(III), and H_2O_2-Cr(III) under different conditions was examined (pH = 6.0–10.0 and molar ratios of PAA to Cr(III)). The degradation rate of TMP by PAA-Cr(III) was greater than by PAA and H_2O_2-Cr(III) under alkaline conditions. Degradation studies using quenching agents and probing molecules, and spectroscopic measurements (UV–visible and electron paramagnetic resonance) suggest $^{\bullet}OH$ as the major radical species and Cr(IV)/Cr(V) as additional reactive species. The oxidized products of TMP by PAA-Cr(III) were identified and possible pathways proposed. Degradation of other pharmaceuticals having different molecular structures by PAA-Cr(III) and H_2O_2-Cr(III) systems were also investigated. Most of the pharmaceuticals degraded at faster rates by PAA-Cr(III) and H_2O_2-Cr(III) than by PAA alone, suggesting that co-present metal ions may play a significant role in PAA oxidation in water treatment.

* Corresponding authors.
E-mail addresses: ching-hua.huang@ce.gatech.edu (C.-H. Huang), vsharma@tamu.edu (V.K. Sharma).

https://doi.org/10.1016/j.jhazmat.2022.129537
Received 10 May 2022; Received in revised form 22 June 2022; Accepted 3 July 2022
Available online 5 July 2022

1. Introduction

Studies on peroxyacetic acid (or peracetic acid) ($CH_3C(O)OOH$, PAA) continue to increase due to its potential as both a disinfectant and an oxidant in treating water. PAA is a promising alternative to chlorination disinfection because of its sterilization ability, feasible implementation, and decreased formation of toxic chlorinated disinfection by-products (DBPs) (Kim and Huang, 2021). PAA has demonstrated remarkable performance in inactivation of viruses, bacteria, and spores and has been applied as a disinfectant in health care facilities and pulp and paper and food industries (Zhang et al., 2020; Sharma et al., 2020; Lee and Huang, 2019). Despite of the high redox potential ($E^0 = 1.0–1.96$ V versus SHE), PAA is not able to degrade recalcitrant pollutants due to its high selectivity. Hence, activation of PAA by UV, metal ions, and activated carbon, has received a lot of attention in recent years to efficiently oxidize organic pollutants (Kim and Huang, 2021). Research is forthcoming on the activation of PAA by low-valent and high-valent transition metal ions to enhance the degradation of pollutants in water, including Fe(II), Co(III), Ru(III), and Fe(VI) (Kim et al., 2019, 2020; Li et al., 2021; Manoli et al., 2022). The results of these studies prompted us to evaluate how the effectiveness of PAA in degrading organic pollutants may be affected by co-present metal ions already in water. The present study examines if the interaction of PAA with chromium(III) (Cr(III)) in water has any role in oxidizing co-existing organic pollutants in water because Cr(III) is often detected in many wastewaters.

Sources of Cr are primarily from industrial wastes such as coal-fired power production, chrome pigment production, wood preservation, stainless steel and cement production, galvanization, electroplating, and leather tanning (Choppala et al., 2013; Deng et al., 2019). Additional input of Cr in wastewater might also be from dietary supplements of Cr (III) (Eastmond et al., 2008; Pradhan et al., 2017). The toxicity of Cr is highly dependent on its oxidation state; Cr(VI) is a known carcinogen but Cr(III) is significantly less toxic (Chen et al., 2019). Reduction of Cr (VI) to Cr(III) has been well-studied (Barrera-Díaz et al., 2012; Xia et al., 2019; Bhati et al., 2019). Trace levels of Cr(III) in wastewater is common and must be carefully dealt with, as oxidation to Cr(VI) has been shown by chlorine, hydrogen peroxide (H_2O_2), and ozone which may produce reactive intermediate complexes of Cr(IV) and Cr(V) (Chebeir and Liu, 2018; Bokare and Choi, 2011; Houshyar et al., 2012; Bell et al., 2021). Significantly, the intermediate Cr species are reactive with organic compounds and may mitigate the treatment of coexisting organic pollutants in water (Bokare and Choi, 2011, 2010; Dong et al., 2020). The standard redox potentials of Cr(V) (E^0 (Cr(V)/Cr(III) = 1.75 V_{NHE}) and Cr(IV) (E^0 (Cr(IV)/Cr(III) = 2.10 V_{NHE}) suggest that Cr-intermediate species may have a role in oxidizing pollutants in water. Therefore, we evaluated whether the co-presence of Cr(III) and PAA could result in such intermediate Cr species and what their roles are in degrading pharmaceuticals in water.

Conventional wastewater treatment processes are ineffective in removing many pharmaceuticals, and a major fraction of these residual pollutants can enter natural water systems, leading to environmental and public health concerns (Jelic et al., 2011; Wang et al., 2020). Antibiotics are among the most prevalent pharmaceuticals in the environment because of their application in human and veterinary medicine along with agricultural purposes (Anquandah et al., 2011; Rizzo et al., 2013). Detected antibiotic concentrations in wastewater effluent have ranged from trace levels to μg/L (Wang et al., 2020; Bijlsma et al., 2021). The primary threats of antibiotics in the environment stem from the potential of altered ecosystems and antibiotic-resistant genes (ARGs) and bacteria (ARB) (Wang et al., 2020; Rizzo et al., 2013; Le et al., 2018). Health concerns surrounding ARGs and ARB arise from a decrease of therapeutic potential against human and animal pathogens (Rizzo et al., 2013). Among the antibiotics, trimethoprim (5-(3, 4, 5-trimethoxybenzyl)pyrimidine-2,4-diamine, TMP) is frequently detected in wastewater effluent and is selected as the model pollutant to perform detailed study (Wang et al., 2020; Bijlsma et al., 2021; Anjali and Shanthakumar, 2019). TMP is often given in pair with sulfonamides to treat various infections (Ji et al., 2016; Masters et al., 2003). A substantial portion of TMP that is excreted in urine maintains its antibiotic properties, whereas only 10–30% is metabolized to an inactive form (Masters et al., 2003). The focus of this study is therefore, on investigating the degradation of TMP during the interaction of PAA with Cr (III). Specifically, we aimed to (i) investigate the interaction between PAA and Cr(III) and the potential of the PAA-Cr(III) system in degrading pharmaceuticals in water, (ii) explore the possible formation of $^{\bullet}OH$, PAA-related radicals ($CH_3C(O)O^{\bullet}$/$CH_3C(O)OO^{\bullet}$), and intermediate Cr species (Cr(IV) and Cr(V)), (iii) identify the main reactive species in the degradation of TMP in the PAA-Cr(III) system, (iv) elucidate the degradation pathways of TMP, and (v) learn if PAA-Cr(III) system degrades other co-existing pharmaceuticals in water with different molecular structures.

2. Experimental methods

2.1. Chemicals and reagents

Trimethoprim (TMP, > 98.0 %), sulfamethoxazole (SMX, > 98.0 %), dexamethasone (DMS, 99.0 %), and enrofloxacin (ENR, > 98.0%) were purchased from Tokyo Chemical Industry (Portland, USA). Atenolol (ATL) was purchased from MP Biomedicals, LLC (Solon, USA). Propranolol hydrochloride (PPN) was purchased from Tocris Bioscience (Bristol, UK). Sodium chromate tetrahydrate (Cr(VI), 99%), peracetic acid solution (PAA, 32 wt% in dilute acetic acid), methanol (HPLC grade, ≥ 99.9 %), carbamazepine (CBZ) was purchased from Sigma-Aldrich (St. Louis, USA). Sodium phosphate dibasic anhydrous, sodium thiosulfate, acetic acid (glacial), o-phosphoric acid (85 %) and L-ascorbic acid (Asc, assay 99.8%) were purchased from Fisher-Scientific (Fair Lawn, USA). Hydrogen peroxide solution (50 %) was purchased from HACH Company World Headquarters (Loveland, USA). Methyl phenyl sulfoxide (PMSO, > 98%) was purchased from Acros Organics (New Jersey, USA) and methyl phenyl sulfone ($PMSO_2$, > 98%) was purchased from Alfa Aesar (Ward Hill, USA). Distilled water used in all solutions in this study were obtained from a Milli-Q Millipore Direct 8 water purification system (> 18.2 MΩ·cm) (Millipore Sigma, Burlington, USA).

2.2. Removal experiments

Initial experimental concentrations of PAA, H_2O_2, acetic acid (AcA), Cr(III), and pollutants were 1315 μM, 520.5 μM, 2055 μM, 13.15 – 1315 μM, and 5.0 μM, respectively. The ratio for $[PAA]_0/[Cr(III)]_0$ ranged from 100 to 1.0. The use of different initial PAA/Cr[III] ratio was to mimic practical conditions in which different amounts of PAA is added to achieve disinfection and treatment. Concentrations of Cr in this study were realistic in wastewater systems, as Cr in industrial wastewater can be up to 3.86 mM (Owlad et al., 2009). Initial concentrations for evaluating TMP degradation in the PAA-Cr(VI) system were $[PAA]_0 = 100.0$ μM, $[Cr(VI)]_0 = 5.0 – 1000.0$ μM, and 5.0 μM TMP. A 10.0 mM Na_2HPO_4 was used as the buffer for all solutions and adjusted to desired pH (6.0–10.0). The use of phosphate buffer allows us to control the speciation of Cr to avoid precipitation. The pH was measured by an Accumet AE150 pH meter (Westford, USA). Samples were taken at different intervals up to 5.0 h, and a 13-mm syringe filter (with 0.2 μm PTFE membrane) was used to remove the insoluble Cr species. These samples were transferred to high-performance liquid chromatography (HPLC) vials and 10.0 μL of 13.0 mM $Na_2S_2O_3$ was added immediately to quench the reaction at desired times. The pollutant concentration in each sample was then analyzed by the HPLC method described in Section 2.4.

The reduction of Cr(VI) by ascorbic acid (Asc) was conducted to identify if Cr-intermediate species may be responsible for TMP degradation. Initial experimental concentrations of Cr(VI), Asc, and TMP were 25.0 – 500.0 μM, 500.0 μM, and 5.0 μM respectively. 10.0 mM Na_2HPO_4

was adjusted to pH 7.0 and used for buffering all solutions. When Asc was used in place of PAA, the Na_2HPO_4 buffer was purged with N_2 for up to 15 min to analyze potential interference of Asc autoxidation with the reduction of Cr(VI); this was analyzed by UV–visible absorbance. Before sample collection for TMP degradation, 10.0 μL of 13.0 mM $Na_2S_2O_3$ was added to all HPLC vials to quench the reaction at desired times.

2.3. Quenching experiments

Radical quenchers were used to probe reactive species present in experiments mentioned above. Benzoic acid (BA) was used to quench $^{\bullet}OH$ and was prepared at an initial concentration of 13.15 mM which was 2360 times higher than pollutant concentration. 5.0 mM of 2,4-hexadiene (2,4-HD) was used to quench both $^{\bullet}OH$ and PAA radicals. Fresh preparation of BA and 2,4-HD were made separately in 10.0 mM Na_2HPO_4 buffered at pH 8.0. Conditions for both BA or 2,4-HD quenching experiments included 1315 μM PAA, 13.15 – 1315 μM Cr (III), and 5.0 μM TMP. Additionally, methyl phenyl sulfoxide (PMSO) can be oxidized to methyl phenyl sulfone ($PMSO_2$) selectively by high-valent metal intermediate species like Cr(V) (Dong et al., 2020). PMSO initial concentration was 200.0 μM, with 263.0 μM Cr(III), and 1315 μM PAA, and samples were collected at every 30 min for 2.0 h.

2.4. Analytical methods

The concentrations of pollutants in samples from the experiments were measured with a Thermo Scientific UltiMate 3000 UHPLC+ with a Restek Ultra C18 5 μm (250 ×4.5 mm) column. Column temperature was maintained at 30 °C for all experiments. Instrument methods for pollutants were as follows in binary mobile phase of solvent A (water with 5% H_3PO_4) and solvent B (methanol): TMP – 75% A and 25% B at flow rate of 1.0 mL·min^{-1} and 271 nm; IBP – 21% A and 79% B at flow rate of 0.8 mL·min^{-1} and 223 nm; ENR – 68% A and 32% B at flow rate of 0.8 mL·min^{-1} and 271 nm; SMX – 60% A and 40% B at flow rate of 0.8 mL·min^{-1} and 290 nm; CBZ – 40% A and 60% B at a flow rate of 0.8 mL·min^{-1} and 284 nm; ATL – 80% A and 20% B at flow rate of 0.8 mL·min^{-1} and 224 nm; DMS – 30% A and 70% B at flow rate of 1.0 mL·min^{-1} and 242 nm; PPN – 45% A and 55% B at a flow rate of 1.0 mL·min^{-1} and 214 nm; PMSO and $PMSO_2$ – 81% A and 19% B at flow rate of 1.0 mL·min^{-1} and 230 nm (PMSO) and 215 nm ($PMSO_2$).

Absorbance analysis using a Thermo Scientific BioMater 3 S UV–visible spectrophotometer was used to monitor the change in absorbance of Cr(III), Cr(VI) and Asc. Measurements were taken for Cr(III) and Cr (VI) at desired times from 0.0 to 2.0 h at different conditions; these conditions depended on concentrations of Cr and PAA as well as pH. In the UV–visible experiment of Cr(VI) and Asc, measurements were taken within 1.0 h for 500.0 μM of both Cr(VI) and Asc at pH 7.0 to compare the effect of purging $N_{2\ (g)}$ into the 10.0 mM phosphate buffer.

A Bruker Elexsys-II E500 electron paramagnetic resonance (EPR) spectrometer equipped with a standard resonator and a CoolEdge cryo system (Billerica, USA) was used to probe the signal of $^{\bullet}OH$. The operating parameters of EPR were: 9.4 GHz frequency (X-band), 20.0 mW microwave power, 9.8 GHz microwave frequency, 1.00 G modulation amplitude, 100 kHz modulation frequency, 120.0 G sweep width, 3340.0 G center field, 30.0 s sweep time, 20 scan times, and 25.0 dB attenuation. The concentration of 5,5-dimethyl-1-pyrroline N-oxide (DMPO, purchased from Sigma-Aldrich (St. Louis, USA)) as the spin trapper for $^{\bullet}OH$ was 50.0 mM. The reaction solutions were injected into a 2-mm quartz EPR tube using a syringe needle, placed into a 4-mm quartz EPR tube, and then measured by EPR immediately.

2.5. Oxidized products (OPs) determination

To identify the OPs of TMP in PAA, PAA-Cr(III), and H_2O_2-Cr(III) systems, 1.0 mL of sample was collected at time = 0.0, 2.0, and 5.0 h of the experiment and purified by solid-phase-extraction (SPE). The Waters Oasis HLB cartridges (WAT106202, 6 cc/200 mg) were first conditioned with 5.0 mL of methanol and 5.0 mL of ultrapure water, respectively. Afterwards, the cartridges were loaded with 1.0 mL of samples from each system. The cartridges were then dried under medium vacuum (15 mmHg) for 10 min, and the TMP and OPs adsorbed on the cartridges were eluted with 1.0 mL of methanol. Untargeted liquid chromatography high resolution mass spectrometry (LC-HRMS) analysis was performed on a Q Exactive Plus Orbitrap mass spectrometer (Thermo Fisher Scientific, Waltham, USA), coupled to a binary pump UltiMate 3000 HPLC with a scan range of m/z 50–1000. The acquired data were processed using Compound Discoverer 3.3 (ThermoFisher Scientific) to screen and identify possible OPs of TMP.

3. Results and discussion

3.1. Degradation of TMP by Cr(III)-PAA system

Initially, experiments were conducted on the degradation of TMP by PAA-Cr(III) at pH 6.0 by varying the concentration of Cr(III) (13.1–1315 μM) while keeping PAA concentration constant at 1315 μM. Similar experiments were also performed using only H_2O_2 because it is inherently present in the solution of PAA (i.e., $CH_3C(O)OH + H_2O_2 \rightleftharpoons CH_3C(O)OOH + H_2O$). As shown in Figs. SM-1 and SM-2, no significant degradation of TMP was observed in all systems. UV–visible absorbance (Fig. SM-2) analysis indicated no Cr(VI) formation.

Next, the pH of the mixed solution of TMP-Cr(III)-PAA was raised to pH 8.0 at a $[PAA]_0$:$[Cr(III)]_0$ molar ratio of 5:1 and the degradation of TMP was followed as a function of time (Fig. 1). Notably, an increase from pH 6.0–8.0 increased the degradation of TMP by both PAA alone and by PAA-Cr(III). However, PAA alone only removed about 20% of TMP in 5.0 h (Fig. 1a), while about 90 % of TMP was degraded by Cr(III)-PAA within the same time (Fig. 1b). This indicates that the increase in pH to alkaline medium had resulted in sufficient reactive species to oxidize TMP. As the pH was increased to 9.0 and 10.0, a slight increase in the degradation of TMP was further observed in both systems (Fig. 1). TMP exhibits two acid dissociation constants ($H_2TMP^{2+} \rightleftharpoons H^+ + HTMP^+$, $pK_{a1} = 3.2$ (Qiang and Adams, 2004); and $HTMP^+ \rightleftharpoons H^+ + TMP$, $pK_{a2} = 7.2$ (Roth and Strelitz, 1969)). In the pH range of 8.0 – 10.0, TMP was mostly present as a neutral species (i.e., 84.2 – 99.9 %). Deprotonated TMP may be more susceptible to oxidation, potentially giving reason to an increase in its degradation from pH 6.0–8.0. PAA has an acid-base equilibrium ($CH_3C(O)OOH \rightleftharpoons H^+ + CH_3C(O)OO^-$; $pK_a = 8.2$) and the fractions of the possible oxidant species of PAA (i.e., $\alpha(CH_3C(O)OOH)$ and $\alpha(CH_3C(O)OO^-)$) vary with pH. For example, $\alpha(CH_3C(O)OOH)$ and $\alpha(CH_3C(O)OO^-)$ at pH 8.0 are 63.1 % and 36.9 %, respectively, which changed to 1.6 % and 98.4 %, respectively, at pH 10.0. It appears that TMP degradation by both oxidant species of PAA was pH independent at the range of 8.0–10.0 (Fig. 1).

The higher degradation efficiency of TMP by PAA-Cr(III) from pH 6.0–8.0 may be attributed to the increasing reactivity of Cr(III) with PAA to yield oxidative species that reacted with TMP (Fig. 1). Chromium(III) exists in different hydroxo species in the acidic to basic pH range. Generally, four hydroxo species, $CrOH^{2+}$, $Cr(OH)_2^+$, $Cr(OH)_3^0$, and $Cr(OH)_4^-$ are present, based on the equilibrium constants (reactions 1–5) (Rai et al., 1987).

$$Cr(OH)_3(s) + 3\ H^+ \rightleftharpoons Cr^{3+} + 3\ H_2O\ K_1 = <9.35 \quad (1)$$

$$Cr(OH)_3(s) + 2\ H^+ \rightleftharpoons CrOH^{2+} + 2\ H_2O\ K_2 = 5.78 \quad (2)$$

$$Cr(OH)_3(s) + H^+ \rightleftharpoons Cr(OH)_2^+ + H_2O\ K_3 < -0.49 \quad (3)$$

$$Cr(OH)_3(s) \rightleftharpoons Cr(OH)_3^{\circ}\ K_4 < -6.84 \quad (4)$$

$$Cr(OH)_3(s) + H_2O \rightleftharpoons Cr(OH)_4^- + H^+\ K_4 < -18.30 \quad (5)$$

A plot of Cr(III) species with pH (Fig. SM-3) suggests that the fractions of $Cr(OH)^{2+}$, $Cr(OH)_2^+$, and $Cr(OH)_3^{\circ}$ are 60%, 30% and 10% at pH

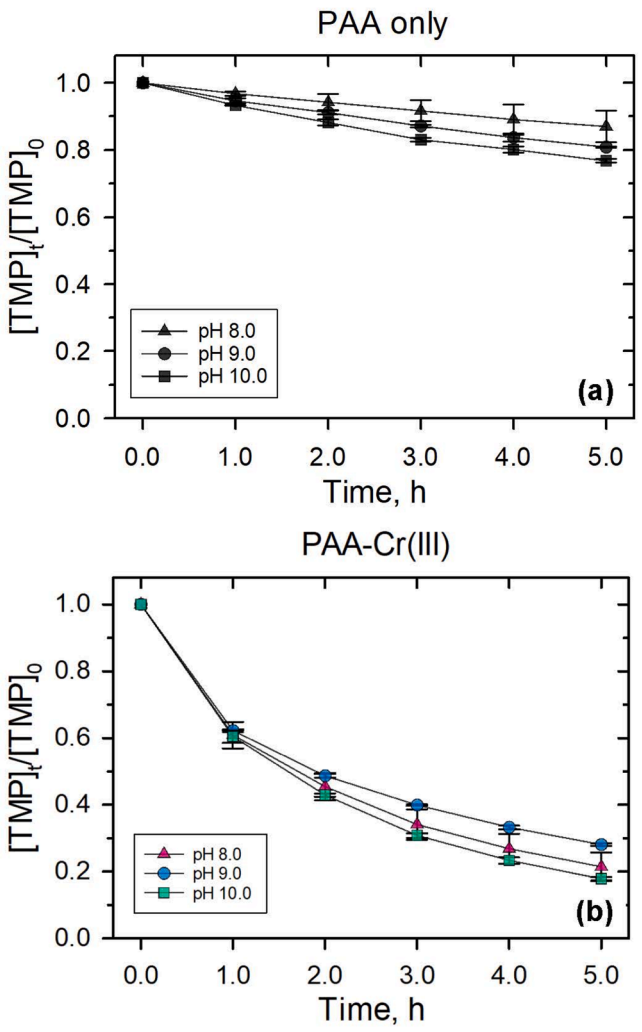

Fig. 1. Degradation of 5.0 μM TMP over 5.0 h at pH 8.0, 9.0, and 10.0 with [Cr (III)]$_0$ = 263.0 μM and [PAA]$_0$ = 1315 μM and [Na_2HPO_4] = 10.0 mM.

6.0. However, at pH 8.0, $Cr(OH)_3^\circ$ is the dominating species (i.e., > 90%) and not much change in this fraction happens when the pH was raised to 9.0 and 10.0 (see Fig. SM-3). It seems that, of the several Cr(III) species present at pH 6.0 ($Cr(OH)^{2+}$, $Cr(OH)_2^+$, and $Cr(OH)_3^\circ$), $Cr(OH)_3^\circ$ could react with PAA to produce reactive species that reacted with TMP. The oxidation of the $Cr(OH)_3^\circ$ appeared to be more thermodynamically feasible than that of other Cr(III) species under acidic condition; consistent with the oxidation of Cr(III) by H_2O_2 in previous studies (Baloga and Earley, 1961; Pettine and Millero, 1990). The reaction rates between $Cr(OH)_3^\circ$ and PAA was not expected to change with pH because the concentration of $Cr(OH)_3^\circ$ does not vary in the pH range of 8.0–10.0. Therefore, degradation of TMP by PAA-Cr(III) in the pH range of 8.0–10.0 did not change significantly at this pH range (see Fig. 1b).

In the next set of experiments, the role of H_2O_2 in PAA was investigated. In this study, the concentration of Cr(III) was varied at pH 8.0 and the degradation of TMP was monitored over 2.0 h (Fig. 2). The H_2O_2-Cr (III) system could also degrade TMP and the maximum degradation was ~40% at a [H_2O_2]$_0$:[Cr(III)]$_0$ molar ratio of 2:1. Comparatively, PAA-Cr (III) degraded ~55% of TMP at a [PAA]$_0$:[Cr(III)]$_0$ molar ratio of 5:1. It should be pointed out that in the mixed solution of PAA and Cr(III) at a molar ratio of 5:1, the molar ratio of H_2O_2 to Cr(III) was 2:1. The results suggest that the PAA-Cr(III) had additional reactive species compared to oxidant(s) in H_2O_2-Cr(III) (Fig. 2).

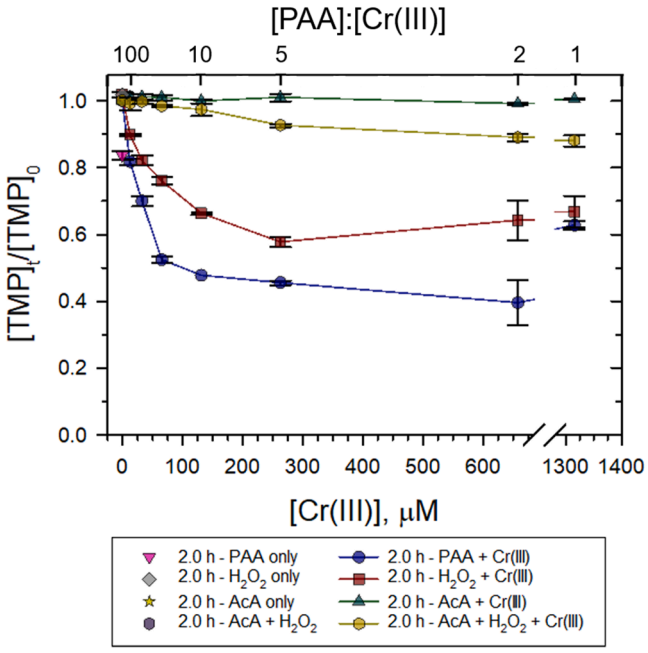

Fig. 2. Degradation of TMP in 2.0 h at pH 8.0 in different systems indicating that PAA-Cr(III) enables greater degradation compared to all other systems. (Experimental condition: [TMP]$_0$ = 5.0 μM, [Cr(III)]$_0$ = 13.15 – 1315 μM, [PAA]$_0$ = 1315 μM, [H_2O_2]$_0$ = 520.5 μM; [AcA]$_0$ = 2.055 mM; [Na_2HPO_4] = 10.0 mM). Note: Experiments were performed using constant PAA (1315 μM) and varied Cr(III) that resulted different molar ratios of [PAA] to [Cr(III)], shown in top y-axis.

3.2. Reactive species study

When PAA interacts with Cr(III), a series of reactions may take place that generate different oxidative species such as Cr(IV), Cr(V), Cr(VI), $^\bullet OH$, $CH_3C(O)O^\bullet$, and $CH_3C(O)OO^\bullet$ (reactions 6–13). The produced reactive species could react with pollutants like TMP (reaction 14).

$$CH_3C(O)OOH + Cr(III) \rightarrow CH_3C(O)O^\bullet + Cr(IV) + OH^- \quad (6)$$

$$CH_3C(O)OOH + Cr(III) \rightarrow CH_3C(O)O^- + Cr(IV) + {}^\bullet OH \quad (7)$$

$$H_2O_2 + Cr(III) \rightarrow Cr(IV) + OH^- + {}^\bullet OH \quad (8)$$

$$CH_3C(O)OOH + Cr(IV) \rightarrow CH_3C(O)O^\bullet + Cr(V) + OH^- \quad (9)$$

$$CH_3C(O)OOH + Cr(IV) \rightarrow CH_3C(O)O^- + Cr(V) + {}^\bullet OH \quad (10)$$

$$H_2O_2 + Cr(IV) \rightarrow Cr(V) + OH^- + {}^\bullet OH \quad (11)$$

$$CH_3C(O)OOH + Cr(V) \rightarrow CH_3C(O)O^\bullet + Cr(VI) + OH^- \quad (12)$$

$$CH_3C(O)OOH + {}^\bullet OH \rightarrow CH_3C(O)OO^\bullet + H_2O \quad (13)$$

$$TMP + {}^\bullet OH/CH_3C(O)O^\bullet/ CH_3C(O)OO^\bullet/Cr(IV)/Cr(V)/Cr(VI) \rightarrow \text{Oxidized products (OPs)} \quad (14)$$

Experiments were performed to determine the main oxidative species involved in the degradation of TMP at pH 8.0. Initially, the formation of Cr(VI) in the mixed PAA and Cr(III) was investigated. The mixed solution had a characteristic spectrum of Cr(VI) (Fig. SM-4) at 372 nm, suggesting the formation of Cr(VI) in the reaction of Cr(III) with PAA (reactions 6–12) (Connett and Wetterhahn, 1985). The reaction of PAA with Cr(III) must be going through the formation of Cr(IV)/Cr(V) prior to the generation of Cr(VI). The formed Cr(VI) may react with TMP. Experiments were then conducted independently by mixing the solutions of Cr(VI) and TMP at pH 8.0. No apparent decrease in the absorbance of Cr(VI) was observed (Fig. SM-5). Furthermore, no significant decrease in the TMP by Cr(VI) mixed solution was observed

(Fig. SM-6). The pH was lowered to 6.0 and 4.0 in this experiment to promote the reduction of Cr(VI), which did not occur and resulted in essentially no TMP degradation. This, along with no significant change in the visible spectra, suggests that Cr(VI) did not oxidize TMP at pH 8.0. Overall, Cr(VI) that was formed in the reaction of Cr(III) with PAA had no role in degrading TMP by PAA-Cr(III) at pH 8.0 (see Fig. 1).

Next, we investigated the possible role of Cr(V)/Cr(IV) in oxidizing TMP. In this set of experiments, we used the known chemistry of Cr(VI) with ascorbic acid (Asc) that generates Cr(V) from the reaction of Cr(VI) + Asc → Cr(V) + Asc$^{\bullet}$ (Goodgame and Joy, 1987; Zhang and Lay, 1996). It is also possible that Cr(V) can react with Asc to yield Cr(IV) (Cr(V) + Asc → Cr(IV) + Asc$^{\bullet}$). Initially, measurements were made to learn if dissolved oxygen in the Asc-Cr(VI) system had a significant impact on the autoxidation of Asc and subsequently the reduction of Cr(VI). $N_{2\ (g)}$ was purged into the system for up to 15 min. The results (Fig. SM-7) indicated almost no change in absorbance at 265 nm (i.e., Asc) and 372 nm (i.e, Cr(VI)) from $N_{2\ (g)}$ purge (noted as "No O_2") over 1.0 h. This suggests that Cr outcompeting the autoxidation of Asc by dissolved oxygen; thus, dissolved oxygen does not interfere with our reaction of Cr (VI) with Asc (Du et al., 2012). Next, TMP was mixed with a solution of Cr(VI) and Asc and the concentration of TMP was monitored over time (Fig. 3). The decrease in TMP was observed, suggesting that formed Cr (V) could react with TMP. It is possible that Cr(V) could also react with Asc to yield Cr(IV), which may also be reacting with TMP. The generated Asc$^{\bullet}$ has usually no reactivity with organic compounds; therefore, both Cr(V)/Cr(IV) may be oxidizing TMP (Bielski, 1982). Results of this study indicate that Cr(V)/Cr(IV) species have a role in oxidizing TMP by PAA-Cr(III).

To determine the contribution of $CH_3C(O)O^{\bullet}/CH_3C(O)OO^{\bullet}$ and $^{\bullet}OH$ in the TMP degradation by the PAA-Cr(III) system, 5.0 mM of 2,4-HD was used as a probe molecule for both species. The C=C double bond in 2,4-HD allows for quenching of acetyl(per)oxyl radicals (i.e., $CH_3C(O)O^{\bullet}$ and $CH_3C(O)OO^{\bullet}$) (Manoli et al., 2022). Notably, a rate constant of 9.2×10^8 $M^{-1}{\cdot}s^{-1}$ was observed between $CH_3C(O)OO^{\bullet}$ and a C=C containing compound (β-carotene) in benzene (Mortensen, 2001). Additionally, the rate constant observed for 2,4-HD and $^{\bullet}OH$ has been reported to be $k = 9.16 \times 10^9$ $M^{-1}{\cdot}s^{-1}$ (Grosjean and Williams, 1992). The use of 2,4-HD in the mixed solution of TMP-PAA-Cr(III) decreased the degradation of TMP (Fig. 4) indicating that both $CH_3C(O)O^{\bullet}/CH_3C(O)OO^{\bullet}$ and $^{\bullet}OH$ species may be contributing to the degradation of TMP. To distinguish between PAA radicals and $^{\bullet}OH$, benzoic acid (BA) was applied to selectively quench $^{\bullet}OH$. BA has much higher reactivity with $^{\bullet}OH$ ($k \approx 4.66 \times 10^9$ $M^{-1}{\cdot}s^{-1}$) than that with $CH_3C(O)OO^{\bullet}$ ($k'_{PAA\bullet} \approx 4.18 \times 10^{-4}$ s^{-1}) (Kim et al., 2020; Wu et al., 2017). As shown in Fig. 4, miniscule difference in the degradation of TMP by the two systems falls within experimental error (i.e., either the addition of 2,4-HD or BA), which suggests that $^{\bullet}OH$ was the dominant oxidant in TMP degradation. It is possible that PAA radicals preferentially reacted with high-valent Cr species like high-valent iron species in the Cr(III)-PAA-TMP system, diminishing their role in oxidizing TMP under the studied experimental conditions (Bielski et al., 1994).

The formation of $^{\bullet}OH$ was further confirmed by EPR in conditions coinciding with our observation of highest TMP degradation. Noted in Fig. 5, no signal was observed for Cr(III), H_2O_2, and PAA solutions alone.

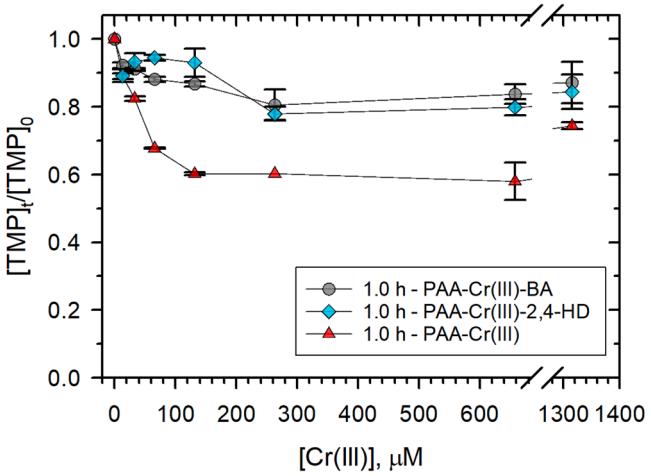

Fig. 4. Degradation of TMP in PAA-Cr(III) system at pH 8.0. Benzoic acid (BA) was added as a quenching agent of $^{\bullet}OH$ and 2,4-hexadiene (2,4-HD) a quenching agent of $^{\bullet}OH$ and PAA radicals. (Experimental conditions: $[TMP]_0 = 5.0$ μM; $[Cr(III)]_0 = 13.15 - 1315$ μM; $[PAA]_0 = 1315$ μM; $[BA]_0 = 13.16$ mM; $[2,4\text{-}HD]_0 = 5.0$ mM; $[Na_2HPO_4] = 10.0$ mM).

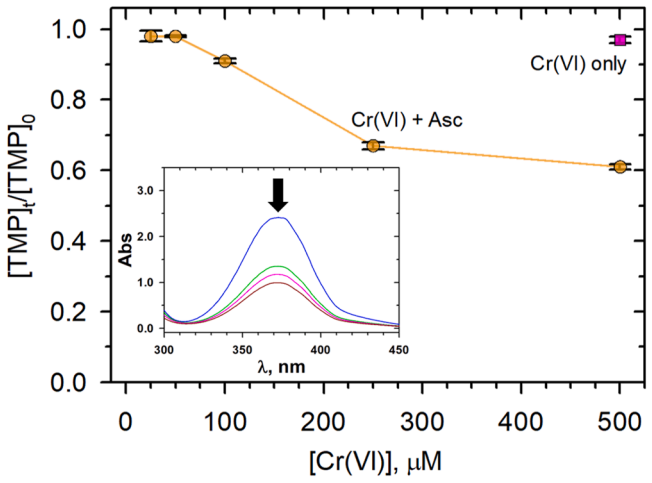

Fig. 3. Degradation of 5.0 μM TMP in 1.0 h at pH 7.0 ($[Na_2HPO_4] = 10.0$ mM) in 500.0 μM ascorbic acid (Asc) and varying $[Cr(VI)]_0 = 25.0 - 500.0$ μM. Inset of UV–visible absorbance showing a decrease in absorbance at 372 nm in 1.0 h under conditions of 500.0 μM Cr(VI) and 500.0 μM Asc at pH 7.0.

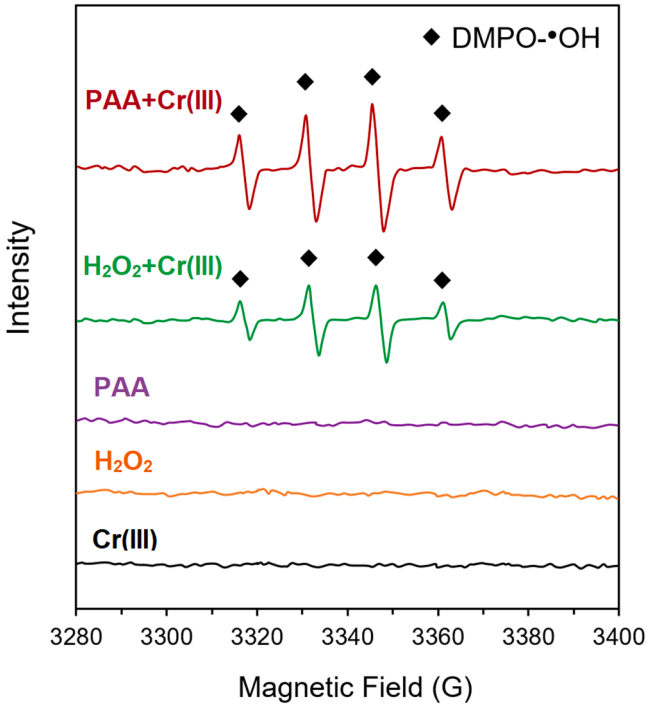

Fig. 5. EPR spectra of DMPO-$^{\bullet}OH$ indicating presence of $^{\bullet}OH$ in both PAA-Cr (III) and H_2O_2-Cr(III) systems at pH 8.0. (Experimental conditions: $[Cr(III)]_0 = 263.0$ μM; $[H_2O_2]_0 = 520.5$ μM; $[PAA]_0 = 1315$ μM; $[DMPO]_0 = 50.0$ mM; $[Na_2HPO_4] = 10.0$ mM).

In contrast, clear signal of the 1:2:2:1 peaks was observed in both the H_2O_2-Cr(III) and PAA-Cr(III) systems, which indicated the formation of DMPO-$^{\bullet}$OH adduct. Significantly, the signal intensity of DMPO-$^{\bullet}$OH was markedly stronger in PAA-Cr(III) than in H_2O_2-Cr(III). This directly relates to Fig. 2, indicating that an increase in TMP degradation by PAA-Cr(III) compared to that of H_2O_2-Cr(III) is primarily due to the more abundant $^{\bullet}$OH.

Lastly, an effort to directly detect Cr-intermediates for the remaining degradation of TMP not attributed to $^{\bullet}$OH was carried out. Oxidation of methyl phenyl sulfoxide (PMSO) to methyl phenyl sulfone ($PMSO_2$) has been used previously to selectively confirm the presence of high-valent metal ion intermediate species such as Fe(V), Ru(V), Co(IV), and Cr(V) (Manoli et al., 2022; Dong et al., 2020; Zong et al., 2021, 2020). The results in Fig. SM-8 indicate that PAA can oxidize PMSO over 2.0 h and appear to have no difference in PMSO oxidation compared to that by PAA-Cr(III). However, from previous experiments, PAA is being consumed in electron transfer steps as Cr(III) becomes oxidized to Cr(VI). Therefore, we expect that oxidation of PMSO by PAA-Cr(III) to be less than that of PAA alone since PAA would be consumed by Cr(III). This indicates that Cr(V) in the PAA-Cr(III) system likely aids in the oxidation of PMSO.

3.3. Oxidized products of TMP

The possible OPs of TMP in the PAA, PAA-Cr(III), and H_2O_2-Cr(III) systems were identified and named after their measured *m/z* values (Figs. SM-9 and SM-10). Based on the literature and detected OPs in this study, the proposed degradation pathways of TMP in these systems were presented in Scheme 1 (Feng et al., 2018; Feng and Sharma, 2018). In the PAA system, hydroxylation is likely the only degradation pathway, which can occur in a step-wise manner to produce OP-306A, OP-322, and OP-338, respectively (Scheme 1*a*). These three OPs were also detected in the PAA-Cr(III) and H_2O_2-Cr(III) systems, along with OP-306B as a new hydroxylated OP (Scheme 1*b*). Notably, the changes in peak areas of these OPs over time showed that hydroxylation of TMP by PAA-Cr(III) was significantly more efficient than by H_2O_2-Cr(III) and PAA alone (Fig. SM-11a-b). This can be attributed to the higher yield of $^{\bullet}$OH in the PAA/Cr(III) system as indicated by the higher signal intensity of DMPO-$^{\bullet}$OH (Fig. 5) because attack by $^{\bullet}$OH often produces hydroxylated products (Qu et al., 2018; An et al., 2014). In both the PAA-Cr(III) and H_2O_2-Cr(III) systems, OP-304 and OP-292 can be formed via H-abstraction and de-methylation, respectively. Both H-abstraction and de-methylation are common reaction pathways between $^{\bullet}$OH and a variety of organic compounds (Acero et al., 2000; Plumlee et al., 2009; Noda et al., 2009; Zhang et al., 2015), however, they are generally unlikely in an un-activated PAA system (Cai et al., 2017; Zhang and Huang, 2020; Zhao et al., 2021). Importantly, the remarkably higher peak areas of various OPs in the PAA-Cr(III) system compared to those in the PAA and H_2O_2-Cr(III) systems (Fig. SM-11a-b) agreed well with the higher degradation efficiency of TMP shown in Fig. 2.

3.4. Degradation of other pharmaceuticals

The PAA-Cr(III) system at pH 8.0 was further explored to determine if other co-pollutants could be degraded. The tested pollutants include sulfamethoxazole (SMX), enrofloxacin (ENR), propranolol (PPN), carbamazepine (CBZ), ibuprofen (IBU), dexamethasone (DMS), and atenolol (ATL). The physicochemical properties of these pollutants including molecular structures are given in Table SM-1. The enhanced degradation of pollutants by PAA-Cr(III) compared to PAA only was observed for all compounds (Fig. 6), again suggesting a role of Cr(III) in generating reactive species through interacting with PAA. Significantly, degradation rates of pollutants by PAA-Cr(III) were either higher than or similar to those by H_2O_2-Cr(III) system. PAA-Cr(III) system could degrade SMX, ENR, PPN, and DMS at faster rates than by H_2O_2-Cr(III), like the degradation of TMP (Fig. 6a). The H_2O_2-Cr(III) system can produce $^{\bullet}$OH through the oxidation of Cr(III) to Cr(VI) (Bokare and Choi, 2011). The H_2O_2-Cr(III) may also generate Cr(IV)/Cr(V) species. The second-order

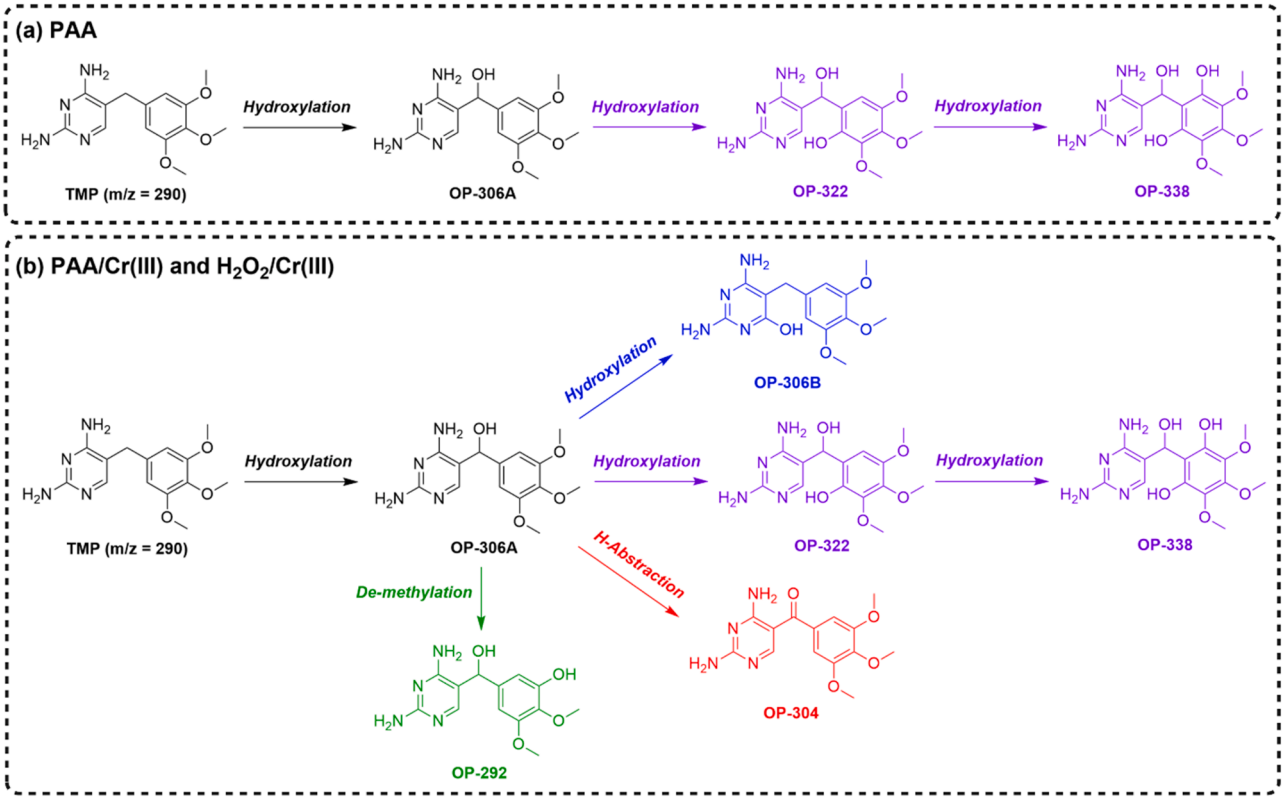

Scheme 1. Proposed degradation pathways of TMP by **(a)** PAA and **(b)** PAA/Cr(III) and H_2O_2/Cr(III).

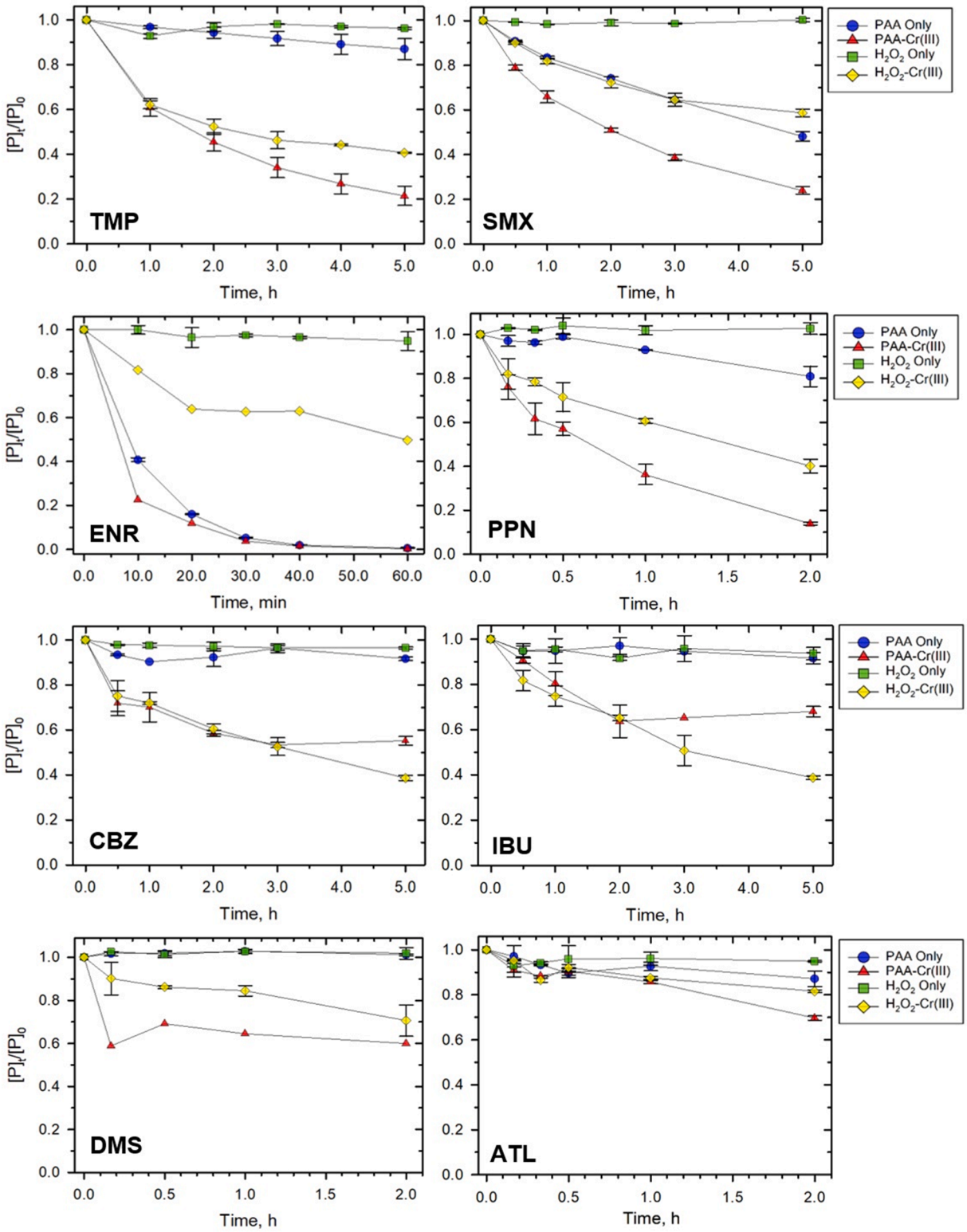

Fig. 6. . Pollutant removal from the reaction between Cr(III) and PAA at pH 8.0. Conditions were: $[P]_0$ = 5.0 μM, $[Cr(III)]_0$ = 263.0 μM, $[PAA]_0$ = 1315 μM, and 10.0 mM phosphate buffer. (TMP = trimethoprim, SMX = tulfamethoxazole, ENR = enrofloxacin, PPN = propranolol hydrochloride, CBZ = carbamazepine, IBU = ibuprofen, DMS = dexamethasone, ATL = atenolol).

rate constants of the reactions between •OH and CBZ, ENR, IBU, SMX, TMP, PPN, and ATL were reported as 8.8×10^9, 8.0×10^9, 6.5×10^9, 5.8×10^9, 6.9×10^9, 1.1×10^{10}, and 7.1×10^9 $M^{-1} \cdot s^{-1}$, respectively (Table SM-2) (McDowell et al., 2005; Santoke et al., 2009; Xiao et al., 2014; Boreen et al., 2004; Dodd et al., 2006; Song et al., 2008). The results of Fig. 6a-d,g indicate the role of additional oxidative species like Cr(V)/Cr(V) in PAA-Cr(III) system. If only •OH, a non-selective oxidant, caused the degradation of TMP, SMX, ENR, and PPN in the PAA-Cr(III) system, similar degradation rates of these pharmaceuticals would be expected. However, observed degradation rates were different and

varied with the type of pharmaceuticals, confirming the presence of additional selective oxidative species. The degradation of the pharmaceuticals in the PAA-Cr(III) systems may be governed by the concentrations of non-selective and selective oxidative species, which may vary with reaction conditions and type of pollutants. The selectivity of Cr(V) has been suggested in degrading a wide range of pollutants by Cr(VI)-S(IV) system (Dong et al., 2020). It is therefore likely the observed degradation of SMX, ENR, and PPN by PAA-Cr(VI) in Fig. 6 was from both $^{\bullet}OH$ and Cr(IV)/Cr(V) species.

Other pharmaceuticals, CBZ, IBU, and ATL were degraded by PAA-Cr(III) and H_2O_2-Cr(III) systems at similar rates (Fig. 6e,f and h). However, rates for both systems were higher than those of PAA or H_2O_2 alone. The second-order reaction rate constants of these pollutants with $^{\bullet}OH$ were similar (Table SM-2). It appears that $^{\bullet}OH$ were largely responsible for degrading these pollutants by both systems and Cr(IV)/Cr(V) species had no apparent role to play in degrading CBZ, IBU, and ATL. This is consistent with the selective nature of high-valent Cr and Fe species to oxidize pollutants, which are derived from the moieties present in the pollutants (Manoli et al., 2022; Dong et al., 2020). Currently, rate constants for the reactions of Cr(IV)/Cr(V) with pollutants are unknown to fully understand their contributions to degrading pollutants in PAA-Cr(III).

4. Conclusions

The study presented herein demonstrated that an addition of PAA to the mild alkaline water containing Cr(III) and TMP resulted in enhanced degradation of TMP. Our results indicated that the primary reactive species responsible for TMP degradation was $^{\bullet}OH$. However, high valent Cr(V) and Cr(IV) were also likely playing a role in the degradation of TMP and other pharmaceuticals. Higher detection of oxidation products in the PAA-Cr(III) system than in the H_2O_2-Cr(III) system provided further evidence of the existence of additional reactive species (Cr(IV)/Cr(V)) in the PAA-Cr(III) system. The inherent presence of H_2O_2 in PAA solution explains somewhat similar observations of TMP degradation in the PAA-Cr(III) and H_2O_2-Cr(III) systems. The advancement of knowledge from this study illustrates how co-existing, redox-active metal ions can work with PAA concertedly in affecting other organic pollutants' oxidative transformation in complicated wastewater matrices.

Environmental Significance

Peracetic acid (PAA) has emerged as an effective oxidant and disinfectant in water treatment, yet how its effectiveness might vary when metal ions and organic molecules co-exist in treatment process is rarely investigated. This study reports for the first time that Cr(III) as a common metal ion in contaminated water could activate PAA to degrade pharmaceuticals in water. We examined interactions of PAA-Cr(III)-pharmaceuticals in detail under various conditions using different experimental approaches to gain insight into involved reactive species including high-valent Cr intermediates, which are generally overlooked. The content presented advanced knowledge of PAA activation and its relevance to water treatment.

CRediT authorship contribution statement

Joshua Bell: Data curation, Methodology, Data analysis, Writing – original draft. **Yinghao Wen:** Data curation, Methodology, Writing – review & editing. **Xingmao Ma:** Writing – review & editing. **Thomas J. McDonald:** Writing – review & editing. **Ching-Hua Huang:** Supervision, Formal analysis, Writing – review & editing. **V. K. Sharma:** Supervision, Formal analysis, Writing – review & editing.

Declaration of Competing Interest

The authors declare that they have no known competing financial interests or personal relationships that could have appeared to influence the work reported in this paper.

Data Availability

Data will be made available on request.

Acknowledgments

The authors, V.K. Sharma and C-H. Huang, wish to thank the support by National Science Foundation Grants CHE 2107967 and CHE 2108701. We thank seven anonymous reviewers for their comments, which improved the paper greatly.

Appendix A. Supporting information

Supplementary data associated with this article can be found in the online version at doi:10.1016/j.jhazmat.2022.129537.

References

Acero, J.L., Stemmler, K., Von Gunten, U., 2000. Degradation kinetics of atrazine and its degradation products with ozone and OH radicals: a predictive tool for drinking water treatment. Environ. Sci. Technol. 34 (4) https://doi.org/10.1021/es990724e.

An, T., Gao, Y., Li, G., Kamat, P.V., Peller, J., Joyce, M.V., 2014. Kinetics and mechanism of •oH mediated degradation of dimethyl phthalate in aqueous solution: experimental and theoretical studies. Environ. Sci. Technol. 48 (1) https://doi.org/10.1021/es404453v.

Anjali, R., Shanthakumar, S., 2019. Insights on the current status of occurrence and removal of antibiotics in wastewater by advanced oxidation processes. J. Environ. Manag. 246, 51–62. https://doi.org/10.1016/j.jenvman.2019.05.090.

Anquandah, G.A.K., Sharma, V.K., Knight, D.A., Batchu, S.R., Gardinali, P.R., 2011. Oxidation of trimethoprim by ferrate(VI): kinetics, products, and antibacterial activity. Environ. Sci. Technol. 45 (24), 10575–10581. https://doi.org/10.1021/es202237g.

Baloga, M.R., Earley, J.E., 1961. The kinetics of the oxidation of Cr(III) to Cr(VI) by hydrogen peroxide [1]. J. Am. Chem. Soc. 83 (24), 4906–4909. https://doi.org/10.1021/ja01485a009.

Barrera-Díaz, C.E., Lugo-Lugo, V., Bilyeu, B., 2012. A review of chemical, electrochemical and biological methods for aqueous Cr(VI) reduction. J. Hazard. Mater. 223–224, 1–12. https://doi.org/10.1016/j.jhazmat.2012.04.054.

Bell, J., Ma, X., McDonald, T.J., Huang, C.-H., Sharma, V.K., 2021. Overlooked role of chromium(V) and chromium(IV) in chromium redox reactions of environmental importance. Environ. Sci. Technol. Water.

Bhati, A., Anand, S.R., Saini, D., Gunture, Sonkar, S.K., 2019. Sunlight-induced photoreduction of Cr(VI) to Cr(III) in wastewater by nitrogen-phosphorus-doped carbon dots. Npj Clean. Water 2 (1), 12. https://doi.org/10.1038/s41545-019-0036-z.

Bielski, B.H., 1982. Chemistry of Ascorbic Acid Radicals. ACS Publications.

Bielski, B.H., Sharma, V.K., Czapski, G., 1994. Reactivity of ferrate (V) with carboxylic acids: a pre-mix pulse radiolysis study. Radiat. Phys. Chem. 44 (5), 479–484.

Bijlsma, L., Pitarch, E., Fonseca, E., Ibáñez, M., Botero, A.M., Claros, J., Pastor, L., Hernández, F., 2021. Investigation of pharmaceuticals in a conventional wastewater treatment plant: removal efficiency, seasonal variation and impact of a nearby hospital. J. Environ. Chem. Eng. 9 (4), 105548 https://doi.org/10.1016/j.jece.2021.105548.

Bokare, A.D., Choi, W., 2010. Chromate-induced activation of hydrogen peroxide for oxidative degradation of aqueous organic pollutants. Environ. Sci. Technol. 44 (19), 7232–7237. https://doi.org/10.1021/es903930h.

Bokare, A.D., Choi, W., 2011. Advanced oxidation process based on the Cr(III)/Cr(VI) redox cycle. Environ. Sci. Technol. 45 (21), 9332–9338. https://doi.org/10.1021/es2021704.

Boreen, A.L., Arnold, W.A., McNeill, K., 2004. Photochemical fate of sulfa drugs in the aquatic environment: sulfa drugs containing five-membered heterocyclic groups. Environ. Sci. Technol. 38 (14), 3933–3940. https://doi.org/10.1021/es0353053.

Cai, M., Sun, P., Zhang, L., Huang, C.H., 2017. UV/Peracetic acid for degradation of pharmaceuticals and reactive species evaluation. Environ. Sci. Technol. https://doi.org/10.1021/acs.est.7b04694.

Chebeir, M., Liu, H., 2018. Oxidation of Cr(III)–Fe(III) mixed-phase hydroxides by chlorine: implications on the control of hexavalent chromium in drinking water. Environ. Sci. Technol. 52 (14), 7663–7670. https://doi.org/10.1021/acs.est.7b06013.

Chen, Q.Y., Murphy, A., Sun, H., Costa, M., 2019. Molecular and epigenetic mechanisms of Cr(VI)-induced carcinogenesis. Toxicol. Appl. Pharmacol. 377, 114636 https://doi.org/10.1016/j.taap.2019.114636.

Choppala, G., Bolan, N., Park, J.H., 2013. Chapter two - chromium contamination and its risk management in complex environmental settings. In: Sparks, D.L. (Ed.), Advances in Agronomy, 120. Academic Press, pp. 129–172. https://doi.org/10.1016/B978-0-12-407686-0.00002-6.

Connett, P.H., Wetterhahn, K.E., 1985. In vitro reaction of the carcinogen chromate with cellular thiols and carboxylic acids. J. Am. Chem. Soc. 107 (14), 4282–4288.
Deng, Y., Wang, M., Tian, T., Lin, S., Xu, P., Zhou, L., Dai, C., Hao, Q., Wu, Y., Zhai, Z., Zhu, Y., Zhuang, G., Dai, Z., 2019. The effect of hexavalent chromium on the incidence and mortality of human cancers: a meta-analysis based on published epidemiological cohort studies. Front. Oncol. 9, 24. https://doi.org/10.3389/fonc.2019.00024.
Dodd, M.C., Buffle, M.-O., von Gunten, U., 2006. Oxidation of antibacterial molecules by aqueous ozone: moiety-specific reaction kinetics and application to ozone-based wastewater treatment. Environ. Sci. Technol. 40 (6), 1969–1977. https://doi.org/10.1021/es051369x.
Dong, H., Wei, G., Cao, T., Shao, B., Guan, X., Strathmann, T.J., 2020. Insights into the oxidation of organic cocontaminants during Cr(VI) reduction by sulfite: the overlooked significance of Cr(V). Environ. Sci. Technol. 54 (2), 1157–1166. https://doi.org/10.1021/acs.est.9b03356.
Du, J., Cullen, J.J., Buettner, G.R., 2012. Ascorbic acid: chemistry, biology and the treatment of cancer. Biochim. Biophys. Acta BBA - Rev. Cancer 1826 (2), 443–457. https://doi.org/10.1016/j.bbcan.2012.06.003.
Eastmond, D.A., MacGregor, J.T., Slesinski, R.S., 2008. Trivalent chromium: assessing the genotoxic risk of an essential trace element and widely used human and animal nutritional supplement. Crit. Rev. Toxicol. 38 (3), 173–190. https://doi.org/10.1080/10408440701845401.
Feng, M., Sharma, V.K., 2018. Enhanced oxidation of antibiotics by ferrate(VI)-sulfur(IV) system: elucidating multi-oxidant mechanism. Chem. Eng. J. 341 https://doi.org/10.1016/j.cej.2018.01.112.
Feng, M., Jinadatha, C., McDonald, T.J., Sharma, V.K., 2018. Accelerated oxidation of organic contaminants by ferrate(VI): the overlooked role of reducing additives. Environ. Sci. Technol. 52 (19) https://doi.org/10.1021/acs.est.8b03770.
Goodgame, D.M.L., Joy, A.M., 1987. EPR study of the Cr(V) and radical species produced in the reduction of Cr(VI) by ascorbate. Inorg. Chim. Acta 135 (2), 115–118. https://doi.org/10.1016/S0020-1693(00)83273-9.
Grosjean, D., Williams, E.L., 1992. Environmental persistence of organic compounds estimated from structure-reactivity and linear free-energy relationships. Unsaturated aliphatics. Atmos. Environ. Part Gen. Top. 26 (8), 1395–1405. https://doi.org/10.1016/0960-1686(92)90124-4.
Houshyar, Z., Khoshfetrat, A.B., Fatehifar, E., 2012. Influence of ozonation process on characteristics of pre-alkalized tannery effluents. Chem. Eng. J. 191, 59–65. https://doi.org/10.1016/j.cej.2012.02.053.
Jelic, A., Gros, M., Ginebreda, A., Cespedes-Sánchez, R., Ventura, F., Petrovic, M., Barcelo, D., 2011. Occurrence, partition and removal of pharmaceuticals in sewage water and sludge during wastewater treatment. Water Res. 45 (3), 1165–1176. https://doi.org/10.1016/j.watres.2010.11.010.
Ji, Y., Xie, W., Fan, Y., Shi, Y., Kong, D., Lu, J., 2016. Degradation of trimethoprim by thermo-activated persulfate oxidation: reaction kinetics and transformation mechanisms. Chem. Eng. J. 286, 16–24. https://doi.org/10.1016/j.cej.2015.10.050.
Kim, J., Huang, C.-H., 2021. Reactivity of peracetic acid with organic compounds: a critical review. ACS EST Water 1 (1), 15–33. https://doi.org/10.1021/acsestwater.0c00029.
Kim, J., Zhang, T., Liu, W., Du, P., Dobson, J.T., Huang, C.-H., 2019. Advanced oxidation process with peracetic acid and Fe(II) for contaminant degradation. Environ. Sci. Technol. 53 (22), 13312–13322. https://doi.org/10.1021/acs.est.9b02991.
Kim, J., Du, P., Liu, W., Luo, C., Zhao, H., Huang, C.-H., 2020. Cobalt/Peracetic acid: advanced oxidation of aromatic organic compounds by acetylperoxyl radicals. Environ. Sci. Technol. 54 (8), 5268–5278. https://doi.org/10.1021/acs.est.0c00356.
Le, T.-H., Ng, C., Tran, N.H., Chen, H., Gin, K.Y.-H., 2018. Removal of antibiotic residues, antibiotic resistant bacteria and antibiotic resistance genes in municipal wastewater by membrane bioreactor systems. Water Res. 145, 498–508. https://doi.org/10.1016/j.watres.2018.08.060.
Lee, W.-N., Huang, C.-H., 2019. Formation of disinfection byproducts in wash water and lettuce by washing with sodium hypochlorite and peracetic acid sanitizers. Food Chem. X 1, 100003. https://doi.org/10.1016/j.fochx.2018.100003.
Li, R., Manoli, K., Kim, J., Feng, M., Huang, C.-H., Sharma, V.K., 2021. Peracetic acid–ruthenium(III) oxidation process for the degradation of micropollutants in water. Environ. Sci. Technol. 55 (13), 9150–9160. https://doi.org/10.1021/acs.est.0c06676.
Manoli, K., Li, R., Kim, J., Feng, M., Huang, C.-H., Sharma, V.K., 2022. Ferrate(VI)-peracetic acid oxidation process: rapid degradation of pharmaceuticals in water. Chem. Eng. J. 429, 132384 https://doi.org/10.1016/j.cej.2021.132384.
Masters, P.A., O'Bryan, T.A., Zurlo, J., Miller, D.Q., Joshi, N., 2003. Trimethoprim-sulfamethoxazole revisited. Arch. Intern. Med. 163 (4), 402–410. https://doi.org/10.1001/archinte.163.4.402.
McDowell, D.C., Huber, M.M., Wagner, M., von Gunten, U., Ternes, T.A., 2005. Ozonation of carbamazepine in drinking water: identification and kinetic study of major oxidation products. Environ. Sci. Technol. 39 (20), 8014–8022. https://doi.org/10.1021/es0500431.
Mortensen, A., 2001. Scavenging of acetylperoxyl radicals and quenching of triplet diacetyl by β-carotene: mechanisms and kinetics. J. Photochem. Photobiol. B 61 (1–2), 62–67. https://doi.org/10.1016/S1011-1344(01)00146-4.
Noda, J., Volkamer, R., Molina, M.J., 2009. Dealkylation of alkylbenzenes: a significant pathway in the toluene, o-, m-, p-Xylene + OH reaction. J. Phys. Chem. A 113 (35). https://doi.org/10.1021/jp901529k.
Owlad, M., Aroua, M.K., Daud, W.A.W., Baroutian, S., 2009. Removal of Hexavalent Chromium-Contaminated Water and Wastewater: A Review. Water Air. Soil Pollut. 200 (1–4), 59–77. https://doi.org/10.1007/s11270-008-9893-7.
Pettine, M., Millero, F.J., 1990. Chromium Speciation in Seawater: The Probable Role of Hydrogen Peroxide. Limnol. Oceanogr. 35 (3), 730–736. https://doi.org/10.4319/lo.1990.35.3.0730.
Plumlee, M.H., Mcneill, K., Reinhard, M., 2009. Indirect photolysis of perfluorochemicals: hydroxyl radical-initiated oxidation of N-ethyl perfluorooctane sulfonamido acetate (N-EtFOSAA) and other perfluoroalkanesulfonamides. Environ. Sci. Technol. 43 (10) https://doi.org/10.1021/es803411w.
Pradhan, D., Sukla, L.B., Sawyer, M., Rahman, P.K.S.M., 2017. Recent bioreduction of hexavalent chromium in wastewater treatment: a review. J. Ind. Eng. Chem. 55, 1–20. https://doi.org/10.1016/j.jiec.2017.06.040.
Qiang, Z., Adams, C., 2004. Potentiometric determination of acid dissociation constants (PKa) for human and veterinary antibiotics. Water Res. 38 (12), 2874–2890. https://doi.org/10.1016/j.watres.2004.03.017.
Qu, R., Li, C., Liu, J., Xiao, R., Pan, X., Zeng, X., Wang, Z., Wu, J., 2018. Hydroxyl radical based photocatalytic degradation of halogenated organic contaminants and paraffin on silica gel. Environ. Sci. Technol. 52 (13) https://doi.org/10.1021/acs.est.8b00499.
Rai, D., Sass, B.M., Moore, D.A., 1987. Chromium (III) hydrolysis constants and solubility of chromium (III) hydroxide. Inorg. Chem. 26 (3), 345–349.
Rizzo, L., Manaia, C., Merlin, C., Schwartz, T., Dagot, C., Ploy, M.C., Michael, I., Fatta-Kassinos, D., 2013. Urban wastewater treatment plants as hotspots for antibiotic resistant bacteria and genes spread into the environment: a review. Sci. Total Environ. 447, 345–360. https://doi.org/10.1016/j.scitotenv.2013.01.032.
Roth, B., Strelitz, J.Z., 1969. Protonation of 2, 4-diaminopyrimidines. I. Dissociation constants and substituent effects. J. Org. Chem. 34 (4), 821–836.
Santoke, H., Song, W., Cooper, W.J., Greaves, J., Miller, G.E., 2009. Free-radical-induced oxidative and reductive degradation of fluoroquinolone pharmaceuticals: kinetic studies and degradation mechanism. J. Phys. Chem. A 113 (27), 7846–7851. https://doi.org/10.1021/jp9029453.
Sharma, N., Bhardwaj, N.K., Singh, R.B.P., 2020. Environmental issues of pulp bleaching and prospects of peracetic acid pulp bleaching: a review. J. Clean. Prod. 256, 120338 https://doi.org/10.1016/j.jclepro.2020.120338.
Song, W., Cooper, W.J., Mezyk, S.P., Greaves, J., Peake, B.M., 2008. Free radical destruction of β-blockers in aqueous solution. Environ. Sci. Technol. 42 (4), 1256–1261. https://doi.org/10.1021/es702245n.
Wang, J., Chu, L., Wojnárovits, L., Takács, E., 2020. Occurrence and fate of antibiotics, antibiotic resistant genes (ARGs) and antibiotic resistant bacteria (ARB) in municipal wastewater treatment plant: an overview. Sci. Total Environ. 744, 140997 https://doi.org/10.1016/j.scitotenv.2020.140997.
Wu, C., De Visscher, A., Gates, I.D., 2017. Reactions of hydroxyl radicals with benzoic acid and benzoate. RSC Adv. 7 (57), 35776–35785. https://doi.org/10.1039/C7RA05488B.
Xia, S., Song, Z., Jeyakumar, P., Shaheen, S.M., Rinklebe, J., Ok, Y.S., Bolan, N., Wang, H., 2019. A critical review on bioremediation technologies for Cr(VI)-contaminated soils and wastewater. Crit. Rev. Environ. Sci. Technol. 49 (12), 1027–1078. https://doi.org/10.1080/10643389.2018.1564526.
Xiao, R., Noerpel, M., Ling Luk, H., Wei, Z., Spinney, R., 2014. Thermodynamic and kinetic study of ibuprofen with hydroxyl radical: a density functional theory approach. Int. J. Quantum Chem. 114 (1), 74–83. https://doi.org/10.1002/qua.24518.
Zhang, L., Lay, P.A., 1996. EPR spectroscopic studies of the reactions of Cr(VI) with L-ascorbic Acid, L-dehydroascorbic acid, and 5,6- *O* -Isopropylidene- L -ascorbic acid in water. [1] Implications for chromium(VI) genotoxicity. J. Am. Chem. Soc. 118 (50), 12624–12637. https://doi.org/10.1021/ja961824c.
Zhang, R., Sun, P., Boyer, T.H., Zhao, L., Huang, C.H., 2015. Degradation of pharmaceuticals and metabolite in synthetic human urine by UV, UV/H2O2, and UV/PDS. Environ. Sci. Technol. 49 (5) https://doi.org/10.1021/es504799n.
Zhang, T., Huang, C.H., 2020. Modeling the kinetics of UV/peracetic acid advanced oxidation process. Environ. Sci. Technol. 54 (12) https://doi.org/10.1021/acs.est.9b06826.
Zhang, T., Wang, T., Mejia-Tickner, B., Kissel, J., Xie, X., Huang, C.-H., 2020. Inactivation of bacteria by peracetic acid combined with ultraviolet irradiation: mechanism and optimization. Environ. Sci. Technol. 54 (15), 9652–9661. https://doi.org/10.1021/acs.est.0c02424.
Zhao, Z., Li, X., Li, H., Qian, J., Pan, B., 2021. New insights into the activation of peracetic acid by Co(II): role of Co(II)-peracetic acid complex as the dominant intermediate oxidant. ACS EST Eng. 1 (10) https://doi.org/10.1021/acsestengg.1c00166.
Zong, Y., Guan, X., Xu, J., Feng, Y., Mao, Y., Xu, L., Chu, H., Wu, D., 2020. Unraveling the overlooked involvement of high-valent cobalt-oxo species generated from the cobalt (II)-activated peroxymonosulfate process. Environ. Sci. Technol. 54 (24), 16231–16239. https://doi.org/10.1021/acs.est.0c06808.
Zong, Y., Zhang, H., Zhang, X., Shao, Y., Zeng, Y., Ji, W., Xu, L., Wu, D., 2021. Highly selective oxidation of organic contaminants in the ruiii-activated peroxymonosulfate process: the dominance of RuVO species. Chemosphere 285, 131544. https://doi.org/10.1016/j.chemosphere.2021.131544.